Biophysical Journal Volume 86 April 2004 2030–2036

Protein Control of Electron Transfer Rates via Polarization: Molecular Dynamics Studies of Rubredoxin

Elizabeth A. Dolan, Robert B. Yelle, Brian W. Beck, Justin T. Fischer, and Toshiko Ichiye
School of Molecular Biosciences, Washington State University, Pullman, Washington 99164-4660

ABSTRACT The protein matrix of an electron transfer protein creates an electrostatic environment for its redox site, which influences its electron transfer properties. Our studies of Fe-S proteins indicate that the protein is highly polarized around the redox site. Here, measures of deviations of the environmental electrostatic potential from a simple linear dielectric polarization response to the magnitude of the charge are proposed. In addition, a decomposition of the potential is proposed here to describe the apparent deviations from linearity, in which it is divided into a "permanent" component that is independent of the redox site charge and a dielectric component that linearly responds or polarizes to the charge. The nonlinearity measures and the decomposition were calculated for *Clostridium pasteurianum* rubredoxin from molecular dynamics simulations. The potential in rubredoxin is greater than expected from linear response theory, which implies it is a better electron acceptor than a redox site analog in a solvent with a dielectric constant equivalent to that of the protein. In addition, the potential in rubredoxin is described well by a permanent potential plus a linear response component. This permanent potential allows the protein matrix to create a favorable driving force with a low activation barrier for accepting electrons. The results here also suggest that the reduction potential of rubredoxin is determined mainly by the backbone and not the side chains, and that the redox site charge of rubredoxin may help to direct its folding.

INTRODUCTION

One of the most intriguing questions in the study of biological electron transfer is how proteins are able to facilitate the long-range electron transfer that occurs in biological systems. Obvious ways are by having recognition sites for specific donors and/or acceptors and by forming complexes, which are both ways of facilitating the optimal formation of the donor-acceptor system. Once the donor-acceptor complex is formed, both the electronic coupling and the nuclear reorganization of the redox site and its environment are important (Devault, 1980; Moser et al., 1992; Gray and Ellis, 1994). Focusing on the latter, the protein provides a certain electrostatic environment for the redox site and changes in the protein matrix can affect the driving force of an electron-transfer reaction (Ichiye, 1999). Although the driving force for the electron transfer reaction can be adjusted by using different cofactors, the substitution of different metals or cofactors does not appear to be a simple way for nature to change reduction potentials. Marcus theory (Marcus and Sutin, 1985) for electron transfer assumes that the activation energy for the electron transfer process is dependent on the energy required to reorganize the environment surrounding the electron donor and acceptor between the reactant and the product states (Fig. 1). This energy is due in large part to the polarization of the environment (i.e., the protein matrix and solvent) around the donor and acceptor redox sites caused by the electrostatic interaction between the redox site charges and the environment.

The environmental response of the protein matrix surrounding the protein redox sites can be compared with the environmental response of the solvent surrounding simple ions. In the case of simple ions in solution, the solvent can freely reorganize around the ions upon electron transfer between two ions, which is a dielectric response that depends on both the polarity of the solvent molecules and the degree of coupling between the molecules. Except in the inverted regime, the large reorganization in a high dielectric solvent such as water gives rise to a large activation energy (Fig. 2 *A*), whereas the small reorganization in a low dielectric solvent gives rise to a small activation energy (Fig. 2 *B*). On the other hand, the protein matrix around the redox site in a protein cannot reorganize freely due to the restraints of the backbone (Fig. 2 *C*). Calculations also indicate a relatively low reorganization energy of the protein for rubredoxin (Ichiye et al., 1995; Yelle et al., 1995), cytochrome *c* (Churg et al., 1983), and the photosynthetic reaction center (Creighton et al., 1988). This implies that the protein is a low dielectric medium. Thus, an electron transfer protein can enhance electron transfer by providing a low dielectric environment for the donor-acceptor complex, which reduces the reorganization energy and thus the activation energy for electron transfer. However, in the case of simple ions in solution, the large solvation energy of a high dielectric solvent such as water can provide a strong driving force for the reaction (Fig. 2 *A*), whereas a low dielectric solvent provides a much weaker driving force (Fig. 2 *B*). Because the protein matrix is a low dielectric medium, the question arises as to how the protein

Submitted June 27, 2003, and accepted for publication December 16, 2003.

Address reprint requests to Dr. Toshiko Ichiye, Dept. of Chemistry, Georgetown University, Washington, DC 20057-1227. Tel.: 202-687-3724; Fax: 202-687-6209; E-mail: ti9@georgetown.edu.

R. B. Yelle's present address is Dept. of Chemistry and Chemical Biology, Harvard University, Cambridge, MA, 02138. Tel.: 617-495-4102; E-mail: yelle@tammy.harvard.edu.

B. W. Beck's present address is Dept. of Biochemistry/MS330, University of Nevada, Reno, Reno, NV 89557-0014. Tel.: 775-784-4183; Fax: 775-784-1419; E-mail: beckbw@unr.edu.

0006-3495/04/04/2030/07 $2.00

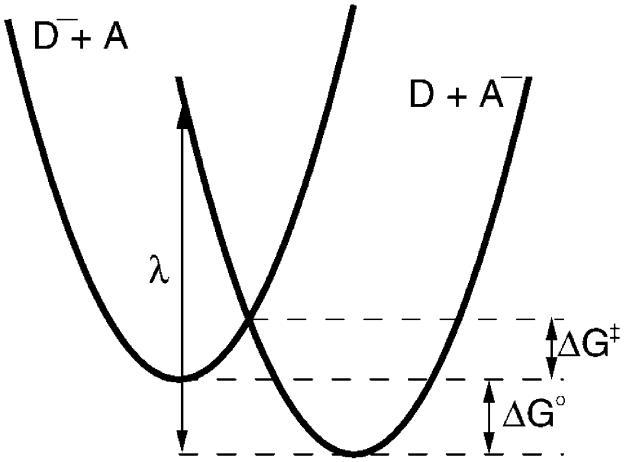

FIGURE 1 A schematic representation of potential energy curves for the electron transfer reaction $D^- + A \rightarrow D + A^-$, where D indicates the donor and A indicates the acceptor, ΔG° is the driving force, $\Delta G^\ddagger$ is the activation energy barrier, and λ is the reorganization energy.

provides sufficient driving force to allow fast electron transfer. The answer may lie in the observation that many proteins appear to have highly polarized environments for their redox sites (Yelle et al., 1995; Swartz et al., 1996; Gunner et al., 1996, 2000), which would influence the reduction potential and thus the driving force. However, it has not been demonstrated whether the electrostatic potential at the redox site is simply the amount expected by introducing a charge equivalent to that of the redox site into a protein matrix that has no intrinsic polarization without the redox site, or if it is actually greater, indicating that the protein has a permanent, charge-independent component to the potential that makes it a better electron acceptor than a redox site analog in a hypothetical solvent of dielectric response equivalent to that of the protein.

The comparison of proteins to simple ions in solution is especially useful because the polarization energy for a simple ion in a dielectric continuum can be simply described by the Born solvation energy, which is a linear response theory and which assumes no permanent potential. Furthermore, relationships can be made between the potential, the fluctuations in the potential, and the dielectric response (Yelle and Ichiye, 1997). Thus, deviations from the Born linear response picture are indications that the protein matrix has more complex behavior than a simple dielectric continuum.

In this work, equations are developed that describe deviations of the polarization response of any media, including a protein, from a linear response, which are based on the Born model for a simple ion in a dielectric continuum. First, measures are developed that indicate apparent deviations from a simple Born linear response. These measures are used to determine the degree of the apparent deviations in the protein rubredoxin using molecular dynamics simulations. Next, because the simplest explanation of a deviation from the simple Born linear response picture in a protein is that there is a permanent potential along with a simple linear dielectric component, a decomposition of the potential into a permanent and a dielectric component is also developed. This decomposition is used to determine the permanent potential in rubredoxin from the molecular dynamics simulations.

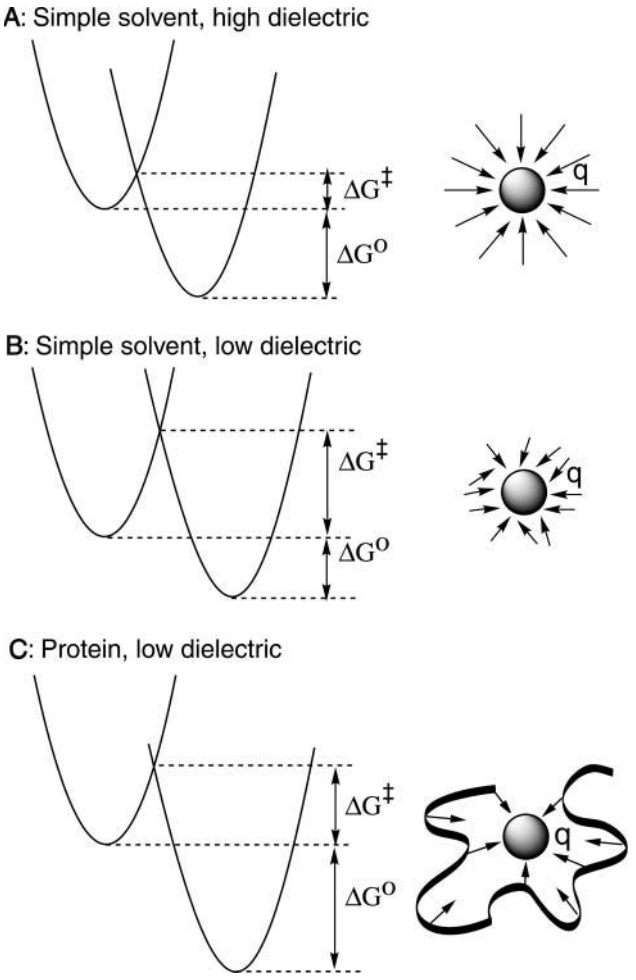

FIGURE 2 A schematic representation of the effects of the environment of the electron acceptor for an electron transfer reaction with $q_D = 1$ and $q_A = 0$. The charge is represented by a circle and the surrounding dipoles are represented by arrows pointing in the direction of their orientation for three types of transfer environments: *(A)* a simple solvent with a high dielectric ($\varepsilon = 80$), where the reorganization is high, as is the driving force for the reaction; *(B)* a simple solvent with low dielectric ($\varepsilon = 4$), where the reorganization is low, as is the driving force of the reaction; and *(C)* a protein, where the reorganization is low due to constraints of the backbone ($\varepsilon = 4$), whereas the driving force is high due to a permanent potential ($\phi_{perm} > 0$).

METHODS

Theory

Here, the energetics of a simple ion in a dielectric continuum followed by that of a protein in solution are reviewed first. Next, the measures of nonlinearity followed by the decomposition are defined.

The energetics of an ion of charge q and radius R in a dielectric continuum with dielectric constant ε is described by the Born solvation free energy

$$\Delta G_q = \frac{-q^2}{2R}\left(1-\frac{1}{\varepsilon}\right), \tag{1}$$

which is due to the polarization of the solvent environment by the charge of the ion. Furthermore, it can be shown that the average solvation energy $\langle V_q\rangle$ is given by

$$\langle V_q\rangle^{(LR)} = \frac{-q^2}{R}\left(1-\frac{1}{\varepsilon}\right), \tag{2a}$$

and the average solvation potential $\langle \phi_q\rangle$ is given by (Hyun et al., 1995)

$$\langle \phi_q\rangle^{(LR)} = \frac{-q}{R}\left(1-\frac{1}{\varepsilon}\right). \tag{2b}$$

The relation $\Delta G = \langle V\rangle/2$ holds because the potential is linear with charge (Ichiye, 1996). Thus, the Born model is a linear response model, as indicated by the superscript (LR). Finally, assuming linear response at temperature T with $\beta = 1/k_BT$ where k_B is Boltzmann's constant, the relationship between the fluctuations in the solvation energy and the dielectric constant ε is given by (Yelle and Ichiye, 1997; Ichiye, 1996)

$$\beta\langle \Delta V_q^2\rangle^{(LR)} = \frac{q^2}{R}\left(1-\frac{1}{\varepsilon}\right), \tag{3a}$$

where $\Delta V = V - \langle V\rangle$ and the relationship between the fluctuations in the solvation potential and the dielectric constant is given by (Yelle and Ichiye, 1997)

$$\beta\langle \Delta \phi_q^2\rangle^{(LR)} = \frac{1}{R}\left(1-\frac{1}{\varepsilon}\right), \tag{3b}$$

where $\Delta\phi = \phi - \langle\phi\rangle$. Thus, in the linear response model, the averages and the fluctuations are not independent quantities and can be related by Eqs. 2 and 3. The energetics of polarization can also be defined when the entire system is described at a molecular level. The redox site can be defined as multiple atoms or sites that all undergo a change in charge upon oxidation or reduction. Also, the environment, which can consist of solvent alone or protein (for example) plus solvent, is also defined in terms of individual atoms or sites. For such cases, an environmental potential energy V_q between the redox site and the environment is defined as

$$V_q = \sum_{i=\text{redox site}}\ \sum_{j=\text{env}} \frac{q_i q_j}{r_{ij}}, \tag{4a}$$

and an environmental potential ϕ_q at the redox site is defined as

$$e\phi_q = -\frac{1}{n}\sum_{i=\text{redox site}}\ \sum_{j=\text{env}} \frac{\Delta q_i q_j}{r_{ij}}, \tag{4b}$$

where r_{ij} is the distance between atoms i and j, Δq_i are the changes in charge of atom i as the redox site is reduced, n is the number of electrons in the reduction (i.e., $n = 1$ for a one-electron reduction), and e is the magnitude of the electron charge. The summation over i is carried out over atoms of the redox site and that over j is carried out over atoms of the rest of the environment. To get average environmental potential energies $\langle V_q\rangle$ and average environmental potentials $\langle\phi_q\rangle$, the quantities in Eq. 4, *a* and *b*, can be calculated from molecular dynamics simulations and then averaged over time or from Monte Carlo simulations and then averaged over configurations.

Here, three measures of the apparent linearity of the response of the environment are defined. These measures utilize the averages and fluctuations of the environmental potential (Eq. 4 *b*) or potential energy (Eq. 4 *a*) from molecular dynamics or Monte Carlo simulations. Moreover, because these numbers can also be predicted from the Born model (Eqs. 2, *a* and *b*, and 3 *a* and *b*), this allows comparison to the ideal case of an ion as a simple linear response solvent with an equivalent ε, assuming that R is constant. Only the environmental potential and not the environmental potential energy is examined here because of the direct relevance to Marcus theory; results for the environmental potential energy are very similar.

First, a measure of whether the potential of the medium at a given charge is consistent with a purely dielectric response is defined here by

$$\chi_q = \frac{\langle\phi_q\rangle}{-q\beta\left\langle\Delta\phi_q^2\right\rangle}. \tag{5}$$

From Eqs. 2 *b* and 3 *b*, $\chi_q < 1$ implies that the potential is less than expected for a medium with a dielectric response consistent with the fluctuations, whereas $\chi_q > 1$ implies that it is more than expected. This will be referred to as the polarization/dielectric measure. The second two measures provide a means of understanding deviations of χ_q from 1. A measure of whether the potential is linear with charge is defined here by comparing the environmental potentials for two different charge states q and q'

$$\xi^{(1)}_{qq'} = \frac{\langle\phi_{q'}\rangle/q'}{\langle\phi_q\rangle/q}. \tag{6}$$

This will be referred to as the linear polarization measure. From Eq. 2 *b*, if $|q| < |q'|$, $\xi_{qq'}{}^{(1)} < 1$ implies that the potential is increasing slower than a purely linear response, whereas $\xi_{qq'}{}^{(1)} > 1$ implies that it is increasing faster than a purely linear response. In addition, a measure of whether the dielectric response is constant with charge is defined here by comparing the fluctuations in the environmental potentials for two different charge states q and q'

$$\xi^{(2)}_{qq'} = \frac{\langle\Delta\phi_{q'}^2\rangle}{\langle\Delta\phi_q^2\rangle}. \tag{7}$$

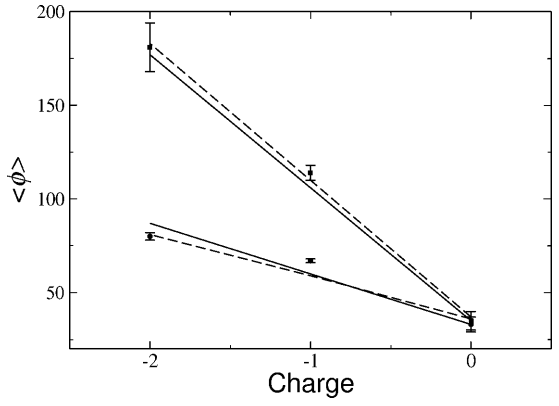

FIGURE 3 The electrostatic potential $\langle\phi\rangle$ in kcal/mol/e as a function of the charge q of the redox site. The $\langle\phi\rangle$ from the molecular dynamics simulations of *C. pasteurianum* rubredoxin are given for the backbone and polar side chains (●) and the total system (■) with error bars. In addition, the linear regression results (*solid line*) and $q = 0$ values (*dashed line*) for ϕ_{perm} and $\beta\psi_\varepsilon{}^2$ (see Table 3) are also shown.

This will be referred to as the constant dielectric measure. From Eq. 3 *b*, if $|q| < |q'|$, $\xi_{qq'}^{(2)} < 1$ implies that the dielectric response is decreasing with charge, whereas $\xi_{qq'}^{(2)} > 1$ implies that is increasing with charge.

Deviations of these three measures from 1 do not necessarily mean that the system is nonlinear. For instance, a special case is when the polarization/dielectric measure $\chi_q > 1$ so that the potential is greater than expected from the fluctuations, the linear polarization measure $\xi_{qq'}^{(1)} < 1$ so that the potential is increasing slower than linearly with charge, and the constant dielectric measure $\xi_{qq'}^{(2)} = 1$ so that the dielectric response is constant with charge. This may be caused by a permanent potential that persists even as the charge $q \rightarrow 0$ in addition to a purely linear polarization due to the dielectric response of the media. In this case, the environmental potential may be decomposed as

$$\langle \phi_q \rangle = \phi_{perm} - q\beta\psi_\varepsilon^2 \tag{8}$$

where the constant ϕ_{perm} is the permanent potential and the constant $\beta\psi_\varepsilon^2$ is the dielectric response factor. In the case of linear response for an ion in a dielectric continuum, $\phi_{perm} = 0$ and $\beta\psi_\varepsilon^2 = (1 - 1/\varepsilon)/R$ by analogy with Eq. 3 *b*. Given data for $\langle \phi_q \rangle$ and $\beta\langle \Delta\phi_q^2 \rangle$, it is possible to solve for ϕ_{perm} and $\beta\psi_\varepsilon^2$ using a linear regression of Eq. 8. For the zero charge case, $\langle \phi_q \rangle = \phi_{perm}$ and $\beta\langle \Delta\phi_q^2 \rangle = \beta\psi_\varepsilon^2$. On the other hand, a deviation of the constant dielectric measure $\xi_{qq'}^{(2)}$ from 1 would indicate that the polarization itself is nonlinear, as may occur if there are protonation changes coupled to the electron transfer.

Molecular dynamics simulations

Molecular dynamics simulations were performed for rubredoxin with a net charge on the redox site $[Fe(SR)_4]$ of 0, −1, and −2, which will henceforth be referred to as $[1Fe]^{0,1-,2-}$, respectively. Coordinates for the oxidized rubredoxin structure from Cp rubredoxin were obtained from the Brookhaven Protein Data Bank (5RXN). For the $[1Fe]^{2-}$, $[1Fe]^{1-}$, and $[1Fe]^0$ rubredoxins, a total of 1835, 1836, and 1837 waters, respectively, were used to solvate the protein, with the addition of 5 Cl^- and 16, 15, and 14 Na^+ counterions, respectively, to neutralize the system. All simulations were performed using CHARMM25 (Brooks et al., 1983) with a potential energy function that combines parameters from CHARMM19 (Brooks et al., 1983) with the TIP3 water model (Jorgensen, 1981) plus additional parameters for the $[1Fe]^{0,1-,2-}$ site (Yelle et al., 1995) and the Na^+ and Cl^- counterions (Hyun and Ichiye, 1997). The partial charges for the $[1Fe]^{0,1-}$ sites are from fits to electrostatic potentials from electronic structure calculations (Mouesca et al., 1994). The partial charges for the $[1Fe]^0$ site were obtained by subtracting the difference in the partial charges between the $[1Fe]^{1-}$ and $[1Fe]^{2-}$ sites from the $[1Fe]^{1-}$ site such that the net charge was zero, whereas the remainder of the energy parameters were the same as the $[1Fe]^{1-}$ site. No explicit electronic polarization was included because the partial charges have been parameterized for the condensed phase environment, allowing the simulations to account implicitly for this feature. Although not exact, Eqs. 2 and 3 indicate that the relationship between the average value and fluctuations of the potential should be consistent. All nonpolar hydrogens were treated via the extended atom model as part of the heavy atom to which they are attached, and all bonds containing hydrogen were held at their equilibrium bond lengths using the SHAKE algorithm (Rychaert et al., 1977).

The simulations were carried out in the microcanonical ensemble with a target temperature of 300 K. The simulations were carried out using the particle mesh Ewald (PME) summation algorithm (Feller, et al., 1996). Cubic boundary conditions of 54 Å × 54 Å × 54 Å were utilized, with a grid spacing equal to 1, a β-spline coefficient equal to 6, and a κ value of 0.34. No atomic polarizability was included and a dielectric constant of one was used throughout the simulations. The time step was 1 fs and the total length of each simulation was 1.16 ns. The last 1 ns of data was analyzed. The reported quantities $\langle \phi \rangle$ and $\beta\langle \Delta\phi^2 \rangle$ were calculated for blocks of 50 ps by averaging ϕ and $\beta\Delta\phi^2$ from coordinates taken at 10-fs intervals and then averaging a total of 20 blocks to yield a total average and a standard deviation for each. The measures of linearity and dielectric response, as well as the decomposition, were calculated from the reported $\langle \phi \rangle$ and $\beta\langle \Delta\phi^2 \rangle$. Errors in the measures and decomposition were calculated from the reported standard deviations of $\langle \phi \rangle$ and $\beta\langle \Delta\phi^2 \rangle$ using standard methods of error propagation.

RESULTS

The averages and fluctuations of the environmental potential, $\langle \phi_q \rangle$ and $\langle \Delta\phi_q^2 \rangle$, respectively, were calculated from the molecular dynamics simulations of rubredoxin (Rd) in the $[1Fe]^{0,1-,2-}$ states for the protein backbone; the protein polar groups, which are the backbone and polar side chains; all polar groups in the system, which include the protein polar groups and solvent; and the entire system (Table 1). The potential due to the polar environment is significant even for $[1Fe]^0$-Rd. For all of the simulations, the similarity of the value of $\langle \phi \rangle$ for just the protein backbone and all of the protein polar groups (backbone plus polar side chains) indicates that the contribution from the polar side chains is small and so the potential is created largely by the backbone. Moreover, the larger value of $\langle \Delta\phi^2 \rangle$ for all polar groups in the system versus the entire system indicates that the contribution of the solvent is correlated with that of the counterions and the charged side chains. In the specific case of the charged side chains, it is important to note that in Cp Rd there are no residues that are titratable at physiological pH (e.g., His). The other charged groups (such as Lys) that occur in Cp Rd are on the surface and solvated, and are thus less likely to be affected by changes in the redox state of the iron. Thus, the contributions of all polar groups in the system will not subsequently be reported independently.

The average value and fluctuations of the environmental potential of the redox site were calculated. The average and fluctuations of the potential of just the backbone or the backbone plus polar side chains are quite similar. However, when water, charged side chains, and counterions are included in addition to the protein, the average value and fluctuations of the potential increase.

The deviations from the linear dielectric response models are given by $\xi_{qq'}^{(1)}$, $\xi_{qq'}^{(2)}$, and χ_q (Table 2). The values of the linear polarization measure $\xi_{qq'}^{(1)}$ indicate that the increase in potential as the charge changes between $[1Fe]^{1-}$-Rd and $[1Fe]^{2-}$-Rd is significantly smaller than expected from linear response. The increase for the backbone and all protein polar groups is much less than linear, whereas the entire system, which includes in addition the charged side chains, counterions, and solvent, is somewhat more linear. The values of the constant dielectric measure $\xi_{qq'}^{(2)}$ for the backbone and all protein polar groups indicate that the dielectric response increases as the charge changes between $[1Fe]^0$-Rd and $[1Fe]^{1-}$-Rd but that the dielectric response decreases as the charge changes between $[1Fe]^{1-}$-Rd and $[1Fe]^{2-}$-Rd. This observation indicates a saturation of the

TABLE 1 Averages $\langle\phi\rangle$ and fluctuations $\beta\langle\Delta\phi^2\rangle$ of the environmental potential for different charge states of the redox site

	$\langle\phi\rangle$				$\beta\langle\Delta\phi^2\rangle$			
Charge	Polar backbone	Polar protein	All polar	Total	Polar backbone	Polar protein	All polar	Total
0	30 ± 3	33 ± 4	57 ± 10	35 ± 5	26 ± 6	27 ± 5	84 ± 24	71 ± 12
−1	63 ± 1	67 ± 1	116 ± 11	114 ± 4	36 ± 7	37 ± 8	173 ± 138	123 ± 28
−2	78 ± 2	80 ± 2	159 ± 14	181 ± 13	20 ± 5	22 ± 5	161 ± 92	138 ± 46

Shown in kcal/mol/e for just the protein backbone (polar backbone), the protein backbone plus polar side chains (polar protein), all of the polar protein plus the water (all polar), and the entire system including charged side chains and counterions (total).

response of the protein with increasing field. However, even given the possible changes in the dielectric response, the polarization/dielectric measure χ_q indicates that the potential of the polar part of the protein is larger than expected from the values of the fluctuations whereas the potential of the entire system is consistent with the fluctuations

Finally, the decomposition of the protein into a permanent and a dielectric component, ϕ_{perm} and $\beta\psi_\varepsilon^2$, respectively, was performed (Table 3). For the protein polar groups, the linear regression results clearly indicate a ϕ_{perm} of 36 kcal/mol/e and a $\beta\psi_\varepsilon^2$ of 23 kcal/mol/e, which are consistent with the results when $q = 0$; i.e., $\langle\phi_{q=0}\rangle = 33$ kcal/mol/e and $\beta\langle\Delta\phi^2_{q=0}\rangle = 27$ kcal/mol/e. For the total system, the linear regression and the $q = 0$ are also consistent so that $\phi_{perm} \approx \langle\phi_{q=0}\rangle$ and $\beta\psi_\varepsilon^2 \approx \beta\langle\Delta\phi^2_{q=0}\rangle$. Interestingly, the results for the total system are similar to the protein polar groups for ϕ_{perm} and only slightly larger for $\beta\psi_\varepsilon^2$.

DISCUSSION

The results presented here for the protein backbone and for all protein polar groups clearly indicate that the protein environment creates a potential that is larger than expected from a simple linear response model. Moreover, they indicate that the protein environment creates a potential that is greater than expected from the fluctuations in the potential, which implies that the potential is greater than expected from the dielectric response properties. Although there are many possible explanations for this, including many different nonlinear effects, the large nonzero $\langle\phi\rangle$ from the protein polar groups in the $[1Fe]^0$-Rd simulation indicates a permanent potential. Also, the similarity of $\langle\phi\rangle$ for the protein polar groups to that of the entire system when the redox site is uncharged (Table 1) indicates that the permanent potential is in the protein. The results for the decomposition into a simple permanent plus linear dielectric component are consistent with this explanation. These results are also consistent with preliminary results for the [4Fe-4S] ferredoxins and high potential iron-sulfur protein (Beck, 1997; Ichiye, 1999). In what follows the implications of these results for electron transfer and folding are discussed.

TABLE 2 Measures of linear dielectric response

Measure	Polar backbone	Polar protein	Total
$\xi^1_{(-1\rightarrow-2)}$	0.62 ± 0.01	0.59 ± 0.01	0.80 ± 0.01
$\xi^2_{(0\rightarrow-1)}$	1.40 ± 0.02	1.37 ± 0.08	1.72 ± 0.09
$\xi^2_{(-1\rightarrow-2)}$	0.55 ± 0.02	0.59 ± 0.01	1.12 ± 0.06
χ_{-1}	1.75 ± 0.33	1.81 ± 0.37	0.93 ± 0.17
χ_{-2}	1.98 ± 0.49	1.85 ± 0.33	0.66 ± 0.17

Shown for just the protein backbone (polar backbone), the protein backbone plus polar side chains (polar protein), and the entire system including charged side chains and counterions (total). Numbers in parentheses indicate charge change.

Implications for reduction potentials

The results here indicate that the permanent potential of the protein apparently is due mainly to the backbone, because little difference is seen between results for just the backbone versus the backbone plus side chains. This is consistent with experimental and theoretical observations that homologous proteins with the same redox site generally have similar reduction potentials, but that specific side chains may cause slight changes (Ichiye, 1999). These observations have led to the picture that the overall three-dimensional fold of the backbone determines the gross value of the reduction potential due to the sequence-dependent positions of the backbone polar groups whereas the side chains can tune the reduction potential, much as the fold determines the basic function of a variety of proteins whereas the side chains can modify the function.

Implications for electron transfer

The overall model of a permanent plus linear dielectric potential has important implications for understanding the electron transfer properties of these proteins. The overall free energy for a one-electron transfer reaction may be written as

$$\Delta G^\circ = G_{DA^-} - G_{D^-A} = \Delta G_\varepsilon{}^\circ - e\phi_{perm}, \tag{9}$$

where acceptor A has a permanent potential ϕ_{perm} (assumed positive here) and $\Delta G^\circ_\varepsilon$ is the free energy due to the dielectric response (Fig. 1). Therefore, the larger the ϕ_{perm}, the more favorable is the reaction. Another important factor for an electron transfer reaction is the activation energy, which may be written as

$$\Delta G^\ddagger = (\lambda + \Delta G^\circ)^2/4\lambda, \tag{10}$$

TABLE 3 Decomposition of potential by linear regression and from $q = 0$ values

	ϕ_{perm}			$\beta\psi_\varepsilon^2$		
Method	Polar backbone	Polar protein	Total	Polar backbone	Polar protein	Total
Linear regression	33 ± 7	36 ± 6	37 ± 5	24 ± 3	23 ± 6	73 ± 5
$q = 0$	30 ± 3	33 ± 4	35 ± 5	26 ± 6	27 ± 5	71 ± 12

Shown in kcal/mol/e for just the protein backbone (polar backbone), the protein backbone plus polar side chains (polar protein), and the entire system including charged side chains and counterions (total).

where

$$\lambda = \Delta G\{\boldsymbol{r}_{D^-+A}; \boldsymbol{q}_{D+A^-}\} - \Delta G\{\boldsymbol{r}_{D+A^-}; \boldsymbol{q}_{D+A^-}\}, \quad (11)$$

is the environmental reorganization energy (Fig. 1), and where $\boldsymbol{r}$ and $\boldsymbol{q}$ denote the set of all coordinates and charges for the system indicated in the subscript. Because λ is independent of ϕ_{perm}, $\lambda = \lambda_\varepsilon$ where the subscript ε indicates that it is solely due to the dielectric response. The activation energy may thus be written as

$$\Delta G^\ddagger = \frac{(\lambda_\varepsilon + \Delta G^\circ_\varepsilon - e\phi_{perm})^2}{4\lambda_\varepsilon}. \quad (12)$$

Therefore, the larger the permanent potential is (as long as $e\phi_{perm} < \lambda_\varepsilon + \Delta G^\circ_\varepsilon$), the smaller the activation energy. Eqs. 11 and 14 together imply that a large permanent potential can increase the favorable driving force while also increasing the reaction rate for the reaction.

The physical interpretation of the above can be made (DeVault, 1980) by assuming a Born-type model for the solvation of D and A independently, with the radii R_D and R_A independent of charge state and with q_D and q_A as the charge state of D after the transfer and of A before the transfer, respectively,

$$\Delta G^\circ_\varepsilon = \frac{1}{2}\left[\frac{-2q_D + 1}{R_D} + \frac{2q_A - 1}{R_A}\right]\left[1 - \frac{1}{\varepsilon}\right], \quad (13)$$

so that

$$\lambda_\varepsilon = \left[\frac{q_D}{R_D} - \frac{q_A - 1}{R_A}\right]\left[1 - \frac{1}{\varepsilon}\right], \quad (14)$$

and

$$\Delta G^\ddagger = \frac{\left[\left(\frac{1}{2R_D} + \frac{1}{2R_A}\right)\left(1 - \frac{1}{\varepsilon}\right) - e\phi_{perm}\right]^2}{4\left[\frac{q_D}{R_D} - \frac{q_A - 1}{R_A}\right]\left[1 - \frac{1}{\varepsilon}\right]}. \quad (15)$$

First, consider the case of no permanent potential, $\phi_{perm} = 0$, such as for two free ions A and D in solution with $q_A \leq 0$ and $q_D \geq 0$. The free energy of the reaction $\Delta G^\circ_\varepsilon$ will decrease with increasing ε, so that the reaction is favored in a high ε_w such as in water, over a low dielectric ε_p such as found inside a protein. However, the environmental reorganization λ_ε will increase with the increasing ε so that the rate of the reaction is slower in a high ε_w over a low dielectric ε_p (Fig. 2, *A* or *B*).

Next, consider the case of a permanent potential $\phi_{perm} > 0$ with a low dielectric ε_p such as for A and D in a protein with $q_A \leq 0$ and $q_D \geq 1$. The free energy ΔG° will decrease with increasing ϕ_{perm} except in the inverted region so that the reaction is favored by the permanent potential over a reaction in the same low dielectric without a permanent potential. However, $\Delta G^\ddagger$ will also decrease with increasing ϕ_{perm} so that the rate of the reaction is even faster with a permanent potential than a reaction in the same low dielectric without a permanent potential, which is already fast compared to a high dielectric. Thus, the permanent potential can help overcome the low driving force found in the low relative to high dielectric media without sacrificing the low reorganization energy of the low relative to high dielectric media and actually enhance it over the low dielectric rate.

Implications for protein folding

These findings also lead to speculations as to how the permanent potential arises. One possibility is that it is inherently built into the amino acid sequence of the protein. Another possibility is that the potential arises during folding around the redox site. In this model, the charged redox site forms at a stage sometime before the protein is fully folded. At this point, which may be a molten globule state, the protein will behave more like a liquid, such as *N*-methylacetamide ($\varepsilon = 179$, $\mu = 4.0$ D) or formamide ($\varepsilon = 109$, $\mu = 3.73$ D), than in the fully folded form, where the dielectric fluctuations are restrained by hydrogen bonds, etc., giving rise to a lower dielectric.

In this higher dielectric state, the protein would polarize more than it would be based on the folded protein dielectric value. Then, hydrogen bonds would form that lock in this potential and lower the dielectric. This model supposes formation of the metal site before complete folding. It would be of interest to examine the potential of metal proteins that can fold without the prosthetic group and/or have large redox sites such as hemes, since the studies here and elsewhere have been done on Fe-S proteins (Beck, 1997; Ichiye, 1999), which have relatively small redox sites.

CONCLUSIONS

The results presented here demonstrate that rubredoxin has a large positive potential of the protein environment around the redox site created mainly by the polar backbone, that rubredoxin has a permanent component to this potential persisting even as the charge of the site goes to zero, and that rubredoxin has a relatively constant dielectric response.

One implication of these results is that the reduction potential of rubredoxin is determined mainly by the backbone and not the side chains. A second implication of these results is that rubredoxin is a good electron acceptor because it has both a low dielectric environment, which keeps the activation energy low, and a permanent potential, which increases the driving force relative to simple dielectric solvents with no permanent potential. A final implication is that the redox site charge might help to direct the folding of this protein.

This work was supported by grants from the National Science Foundation (MCB9808116) and the National Institutes of Health (GM45303). Computation was performed on a 16-processor IBM SP2 funded by the National Science Foundation (BIR-9512538) and Washington State University. Additional computer time was provided by the Maui High Performance Computing Center (sponsored in part by the Phillips Laboratory, Air Force Materiél Command, USAF, under cooperative agreement number F29601-93-2-0001) and through computing resources provided by the National Partnership for Advanced Computational Infrastructure at the San Diego Supercomputer Center under NSF cooperative agreement ACI-9619020 and MCB990010. The views and conclusions contained in this document are those of the authors and should not be interpreted as necessarily representing the official policies or endorsements, either expressed or implied, of Phillips Laboratory or the U.S. government.

REFERENCES

Beck, B. W. 1997. Theoretical investigations of iron-sulfur proteins. PhD (Biochemistry) thesis. Washington State University, Pullman, WA.

Brooks, B. R., R. E. Bruccoleri, B. D. Olafson, D. J. States, S. Swaminathan, and M. Karplus. 1983. CHARMM: a program for macromolecular energy, minimization, and dynamics calculations. *J. Comput. Chem.* 4:187–217.

Churg, A. K., R. M. Weiss, A. Warshel, and T. Takano. 1983. On the action of cytochrome *c*: correlating geometry changes upon oxidation with energies of electron transfer. *J. Phys. Chem.* 87:1683–1694.

Creighton, S., J.-K. Hwang, A. Warshel, W. W. Parson, and J. Norris. 1988. Simulating the dynamics of the primary charge separation process in bacterial photosynthesis. *Biochemistry.* 27:774–781.

Devault, D. 1980. Quantum mechanical tunneling in biological systems. *Q. Rev. Biophys.* 13:387–564.

Feller, S. E., R. W. Pastor, A. Rojnuckarin, S. Bogusz, and B. R. Brooks. 1996. Effect of electrostatic force truncation on interfacial and transport properties of water. *J. Phys. Chem.* 100:17011–17020.

Gray, H. B., and W. R. Ellis, Jr. 1994. Electron transfer. *In* Bioinorganic Chemistry. I. Bertini, H. B. Gray, S. J. Lippard, and J. S. Valentine, editors. University Science Books, Sausilito, CA. 315–363.

Gunner, M. R., A. Nicholls, and B. Honig. 1996. Electrostatic potentials in *Rhodopseudomonas viridis* reaction centers: implications for the driving force and directionality of electron transfer. *J. Phys. Chem.* 100:4277–4291.

Gunner, M. R., M. A. Saleh, E. Cross, A. ud-Doula, and M. Wise. 2000. Backbone dipoles generate positive potentials in all proteins: origins and implications of the effect. *Biophys. J.* 78:1126–1144.

Hyun, J.-K., C. S. Babu, and T. Ichiye. 1995. Apparent local dielectric response around ions in water: a method for its determination and its applications. *J. Phys. Chem.* 99:5187–5195.

Hyun, J.-K., and T. Ichiye. 1997. Understanding the Born radius via computer simulations and theory. *J. Phys. Chem. B.* 101:3596–3604.

Ichiye, T. 1996. Solvent free energy curves for electron transfer: a nonlinear solvent response model. *J. Chem. Phys.* 104:7561–7571.

Ichiye, T. 1999. Computational studies of redox potentials of electron transfer proteins. *In* Simulation and Theory of Electrostatic Interactions in Solution. L. R. Pratt and G. Hummer, editors. AIP, Santa Fe, NM. 431–450.

Ichiye, T., R. B. Yelle, J. B. Koerner, P. D. Swartz, and B. W. Beck. 1995. Molecular dynamics simulation studies of electron transfer properties of Fe-S proteins. *In* Biomacromolecules: From 3-D Structure to Applications. R. L. Ornstein, editor, Pasco, WA. 203–213.

Jorgensen, W. L. 1981. Transferable intermolecular potential functions for water, alcohols, and ethers. Application to liquid water. *J. Am. Chem. Soc.* 103:335–340.

Marcus, R. A., and N. Sutin. 1985. Electron transfer in chemistry and biology. *Biochim. Biophys. Acta.* 811:265–322.

Moser, C. C., J. M. Keske, K. Warncke, R. S. Farid, and P. L. Dutton. 1992. Nature of biological electron transfer. *Nature.* 355:796–802.

Mouesca, J.-M., J. L. Chen, L. Noodleman, D. Bashford, and D. A. Case. 1994. Density functional/Poisson-Boltzmann calculations of redox potentials for iron-sulfur clusters. *J. Am. Chem. Soc.* 116:11898–11914.

Rychaert, J. P., G. Ciccotti, and H. J. C. Berendsen. 1977. Numerical integration of the cartesian equation of motion of a system with constraints: molecular dynamics of n-alkanes. *J. Comput. Phys.* 23:327–341.

Swartz, P. D., B. W. Beck, and T. Ichiye. 1996. Structural origins of redox potential in iron-sulfur proteins: electrostatic potentials of crystal structures. *Biophys. J.* 71:2958–2969.

Yelle, R. B., and T. Ichiye. 1997. Solvation free energy reaction curves for electron transfer: theory and simulation. *J. Phys. Chem. B.* 101:4127–4135.

Yelle, R. B., N.-S. Park, and T. Ichiye. 1995. Molecular dynamics simulations of rubredoxin from *Clostridium pasteurianum*: changes in structure and electrostatic potential during redox reactions. *Proteins.* 22:154–167.